Anal. Chem. **2002,** *74,* 1119−1127

Performances and Limits of a Parallel Oscillator for Electrochemical Quartz Crystal Microbalances

Hervé Ehahoun, Claude Gabrielli, Michel Keddam, Hubert Perrot,* and Philippe Rousseau

UPR15 du CNRS, Physique des Liquides et Electrochimie, Université Pierre et Marie Curie, 4 place Jussieu, 75252 Paris, Cedex 05, France

This paper describes a driving circuit for an electrochemical quartz crystal microbalance (EQCM) adapted to a wide range of applications. The oscillator is a Miller-type parallel oscillator using an operational transconductance amplifier (OTA). A theoretical study of the oscillating circuit led to the analytical expression of the microbalance frequency as well as to an overestimation of the error on the mass measurement. The reliability of the EQCM was then experimentally verified through electrochemical copper deposition and dissolution. The limit of operation of the EQCM was also investigated, both analytically and experimentally. This work shows that parallel oscillators using few electronic components allow a very reliable EQCM to be obtained for mass measurements on metallic films, even if they are highly damped.

Sauerbrey first demonstrated the mass sensitivity of piezoelectric quartz crystals to mass variations of thin films on the crystal surface.[1,2] The quartz crystal microbalance (QCM) is mainly based on an electronic circuit driving an AT-cut quartz crystal resonator. The driving circuit and the quartz resonator constitute an electronic oscillator. Its frequency is expected to follow the frequency shifts of the resonator, induced by the mass variations of the film on the crystal surface.

The driving circuit is of the highest importance, because it critically influences the skills of the entire sensor. Different oscillator circuits have been proposed on the basis of various active components, such as controlled-gain voltage amplifiers,[3] field-effect transistors (FET),[4] TTL circuits,[5] or operational transconductance amplifiers (OTA).[6] Quartz crystal oscillators are commonly separated into two classes: the series oscillators, which follow shifts of the series resonance frequency of the quartz resonator; and the parallel oscillators, whose frequency is close to the antiresonance or parallel frequency of the resonator. In both cases, the driving circuit is affected by a change of the quality factor of the resonator. Investigations have shown that even electrodeposited metallic films can lead to a high damping of the quartz oscillation.[7] This fact questions the reliability of microbalances, even in basic cases of electrochemical studies, like the determination of the faradaic efficiency during a metallic electrodeposition, since high variations in the damping may induce significant shifts of the microbalance frequency independently of effective mass variations at the crystal surface. The possibility of designing reliable series oscillators over a wide range of damping has been successfully investigated.[8] Our purpose is then to propose a rather simple parallel oscillator, also found to be very reliable in many cases of high damping.

Besides the reliability of the gravimetric measurement, the maximum mass or thickness of the film that may be supported by the quartz resonator beyond which microbalance operation fails is important. In many investigations using a microbalance, the studied system was a film initially present on the quartz surface. It was the case, for example, in various corrosion studies of metallic substrates.[9−11] Therefore, the maximum load allowing microbalance operation may influence the characteristics of the investigated system or limit the observation domain. The driving circuit chosen for the microbalance oscillator is, in this point of view, also very important.

In this paper, a Miller-type parallel oscillator is used and both the reliability of the mass measurement and the maximum supported load are analytically and experimentally determined. The derivation is based on the Butterworth−Van Dyke model (BVD) of the quartz crystal resonator from which the microbalance frequency is calculated with respect to the series frequency of the resonator. Experimental microbalance data were compared to measurements of the electroacoustic admittance of the resonator. These electroacoustic data were treated also with regard to the BVD model. A detailed description of this model is found in the related literature.[12−15]

Numerous researchers in chemistry use homemade microbalances, because such devices generally offer a high flexibility and the possibility of adapting the circuit to homemade quartz cells

* Corresponding author. Fax: 33 1 44 27 40 74. E-mail: perrot@ccr.jussieu.fr.

(1) Sauerbrey, G. *Z. Phys.* **1959**, *155*, 206−212.
(2) Sauerbrey, G. *Z. Phys.* **1964**, *178*, 457−471.
(3) Soares, D. M. *Meas. Sci. Technol.* **1993**, *4*, 549−553.
(4) Bruschi, L.; Delfitto, G.; Mistura, G. *Rev. Sci. Instrum.* **1999**, *70* (1), 153−157.
(5) Bruckenstein, S.; Shay, M. *Electrochim. Acta* **1985**, *30* (10), 1295−1300.
(6) Eichelbaum, F.; Borngraber, R.; Schroder, J.; Lucklum, R. *Rev. Sci. Instrum.* **1999**, *70*, 2537−2545.
(7) Wünsche, M.; Meyer, H.; Schumacher, R.; Wasle, S.; Doblhofer, K. *Z. Phys. Chem.* **1999**, *208*, 225−238.
(8) Wessendorf, K. O. *IEEE Int. Freq. Control. Symp. Proc.* **1993**, 711−717.
(9) Yao, S. Z.; Chen, J. H.; Nie, L. H. *Corrosion* **1997**, *53* (3), 195−199.
(10) Aastrup, T.; Wadsak, M.; Schreiner, M.; Leygraf, C. *Corros. Sci.* **2000**, *42*, 957−967.
(11) Ehahoun, H.; Gabrielli, C.; Keddam, M.; Perrot, H.; Cètre, Y.; Diguet, L. J. *Electrochem. Soc.* **2001**, *148*, 333−336.
(12) Kipling, A. L.; Thompson, M. *Anal. Chem.* **1990**, *62*, 1514−1519.
(13) Yang, M.; Thompson, M. *Anal. Chem.* **1993**, *65*, 1158−1168.
(14) Martin, S. J.; Frye, G. C.; Ricco, A. J.; Senturia, S. D. *Anal. Chem.* **1993**, *65*, 2910−2922.
(15) Arnau, A.; Sogorb, T.; Jiménez, Y. *Rev. Sci. Instrum.* **2000**, *71* (6), 2563−2571.

10.1021/ac010883s CCC: $22.00
Published on Web 01/29/2002

Table 1. Summary of the Relevant Frequencies for the Theoretical Analysis

ω_s	series resonant frequency of the quartz	maximizes Re[$Y_q(\omega)$]
ω_p	parallel resonant frequency of the quartz	upper root of Im[$Y_q(\omega)$] at $R_m = 0$
Ω_s	series zero-phase frequency of the quartz	lower root of Im[$Y_q(\omega)$] (at $R_m \neq 0$, associated to ω_s)
Ω_p	parallel zero-phase frequency of the quartz	upper root of Im[$Y_q(\omega)$] (at $R_m \neq 0$, associated to ω_p)
ω_μ	microbalance frequency of the oscillator	frequency of the electronic oscillator when controlled by the resonator
ω_{rest}	rest frequency of the oscillator	frequency of the electronic oscillator when no longer controlled by the resonator

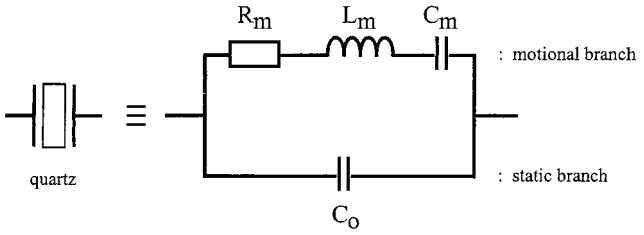

Figure 1. Classical BVD equivalent circuit for a quartz resonator.

designed for their specific applications. The proposed circuit is relatively simple and has just a few components. It can be built in only a few hours, but it is highly reliable for a wide range of applications and can be easily modified. The analytical presentation of its functioning does not refer to complicated notions of electronics. The calculations are based, on one hand, on the equivalent circuit of the quartz, and on the other hand, on the two conditions of Barkhausen that are also two basic equations of electronics. From these few equations, the main aspects of the device's functioning are obtained through rather simple mathematics, because the most complex step is the resolution of a second-order linear equation.

Our purpose is to propose a simple microbalance circuit that we believe to have a good experimental behavior, even for high-mass loads. On changing the values of the electronic components (and the involved cutoff frequencies), it may be possible to obtain many functioning configurations. We show in this paper one configuration found to be very satisfying. This does not mean that other configurations are not possible; however, the proposed calculations are valid only for the configuration shown here. They can obviously be used as the basis for the analytical treatment of derived configurations.

THEORY

In this paper, the Greek letters ω and Ω are used for angular frequencies (unit: rad s^{-1}) and the Latin letters f and F for frequencies (unit: Hz). Frequencies and angular frequencies are related by the classical relationship: $\omega = 2\pi f$. To lighten many equations, angular frequencies are here simply called frequencies, considering the Greek letters as significant enough. The notation for the six relevant frequencies is shown in Table 1. For each frequency, the definition and the meaning will be given again when one of them is introduced in the course of this theoretical analysis.

An equivalent circuit is associated with the quartz crystal in order to explain its behavior when inserted in an electronic oscillator (cf. Figure 1).[13] The quartz series frequency, ω_s, is given by

$$\omega_s = \frac{1}{\sqrt{L_m C_m}} \qquad \text{that is, } L_m C_m \omega_s^2 = 1 \tag{1}$$

where L_m, C_m, and R_m are the components of the motional arm and C_p is the parallel capacitance of the resonator (Figure 1).

For ideal layers without losses, the change of ω_s is proportional to the mass of the deposited layer over a wide range of mass load.[1,2] For higher loads, nonlinearity appears, and the mass calculation should include a correction, as shown by Lu and Lewis.[16] The admittance Y_q of the equivalent circuit of the quartz is[13]

$$Y_q(\omega) = jC_p\omega + \frac{1}{R_m + jX_m(\omega)} \tag{2}$$

where C_p is the effective parallel capacitance (including C_0, the static capacitance of the quartz alone, and parasitic capacitances due to the electric connections of the quartz), and

$$X_m(\omega) = L_m\omega - \frac{1}{C_m\omega} \tag{3}$$

For an ideal quartz without losses ($R_m = 0$), the imaginary part of this admittance is zero at a frequency called *quartz parallel frequency*, ω_p, whose expression is[14]

$$\omega_p = \omega_s\sqrt{1 + \frac{C_m}{C_p}} \approx \omega_s\left(1 + \frac{C_m}{2C_p}\right) \tag{4}$$

because $C_m \ll C_p$.

The spectrum of the quartz admittance shows two zero-phase frequencies, Ω_s and Ω_p, respectively called *series* and *parallel zero-phase frequencies* of the quartz, such as[17]

$$\Omega_{p/s} = \frac{\omega_s + \omega_p}{2} \pm \frac{1}{2}\sqrt{(\omega_s - \omega_p)^2 - \frac{R_m^2}{L_m^2}} \tag{5}$$

For an ideal quartz without losses, $\Omega_{p/s}(R_m = 0) = \omega_{p/s}$.

Open-Loop Gain of the Oscillator; Conditions of Barkhausen. For an oscillator of the Pierce family[18] schematized in Figure 2a with a transistor T, the open loop gain A_L is equal to

$$A_L = -g_m \frac{Z_1 Z_2}{Z_1 + Z_2 + Z_3} \tag{6}$$

(16) Lu, C.; Lewis, O. *J. Appl. Phys.* **1972**, *43*, 4385.
(17) Soares, D. M.; Kautek, W.; Fruböse, C.; Doblhofer, K. *Ber. Bunsen-Ges. Phys. Chem.* **1994**, *98* (2), 219−228.
(18) Parzen B. *Design of Crystal and Other Harmonic Oscillators*; Wiley−Interscience: New York, 1983.

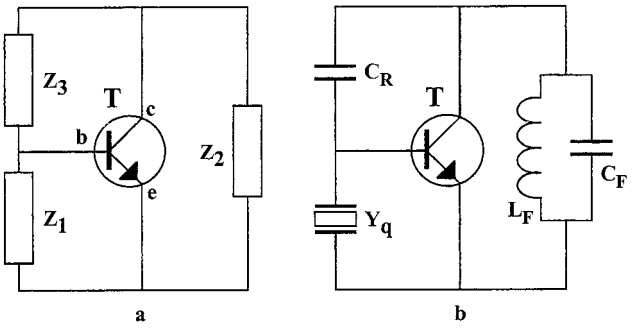

Figure 2. Schematic representation of two oscillators: (a) Pierce and (b) Miller.

where g_m is the transistor transconductance (in general, a complex quantity varying with the frequency), or using the admittances

$$A_L = -g_m \frac{Y_3}{Y_2Y_3 + Y_1Y_3 + Y_1Y_2} \quad (7)$$

where $Y_i = 1/Z_i$.

The oscillator discussed in this study is a Miller quartz crystal oscillator. The quartz resonator is inserted in branch 1 (cf. Figure 2b). By taking into account the input and output impedances of the transistor, the various admittances Y_1, Y_2, and Y_3 are equal to

$$Y_1(\omega) = Y_q(\omega) + jC_{in}{}^T\omega = jC_p{}'\omega + \frac{1}{R_m + jX_m(\omega)} \quad (8)$$

where $C_{in}{}^T$ is the input capacitance of the transistor, and $C_p{}' = C_p + C_{in}{}^T$.

Besides,

$$Y_2(\omega) = G_{out}{}^T + j\left(C_F{}'\omega - \frac{1}{L_F\omega}\right) \quad (9)$$

where $G_{out}{}^T$ is the transistor output conductance. C_F and L_F are the capacitance and inductance of the band-pass filter. $C_F{}'$ takes into account the transistor output capacitance, $C_{out}{}^T$, represented by $C_F{}' = C_F + C_{out}{}^T$. In this paper, the components of the band-pass filter were chosen so that the cutoff frequency, ω_F, defined by $L_FC_F{}'\omega_F{}^2 = 1$, was lower than the quartz series frequency ($\omega_F < \omega_q$. It was experimentally observed that the oscillator could also work with a ω_F higher than ω_s, but no significant enhancement of the oscillator skills was noticed in this case).

In addition,

$$Y_3(\omega) = jC_R\omega \quad (10)$$

where C_R is the capacitor used for the reaction loop, here referred to as reaction capacitance.

According to the Barkhausen conditions of oscillation,[18] the circuit oscillates if the real and imaginary parts of the open loop gain satisfy

$$\mathrm{Im}[A_L(\omega)] = 0 \quad (11)$$

and

$$\mathrm{Re}[A_L(\omega)] \geq 1 \quad (12)$$

The first relationship gives the oscillation frequencies, and the second relationship gives the condition to start oscillation. In the following, the transistor considered is an operational transconductance amplifier with real and constant transconductance over a range exceeding the frequencies involved in this paper. Such integrated circuits have been shown to be adapted for microbalance electronic design.[6] Then, as $\mathrm{Re}[Y_3(\omega)] = 0$, the first condition of oscillation becomes

$$\mathrm{Re}[Y_2Y_3 + Y_1Y_3 + Y_1Y_2] = 0 \quad (13)$$

Equation 13 can be written under the following form

$$(\Gamma_F(\omega) + C_R\omega)[\bar{C}_p(\omega)\omega(R_m{}^2 + X_m{}^2(\omega)) - X_m(\omega)] = G_{out}{}^T R_m \quad (14)$$

where $X_m(\omega) = L_m\omega - 1/C_m\omega$ (term associated to the crystal series resonance), $\Gamma_F(\omega) = C_F{}'\omega - 1/L_F\omega$ (term associated to the band-pass filter cutoff), $\bar{C}_p(\omega) = C_p{}' + \Gamma_F(\omega)/\Gamma_F(\omega) + C_R\omega C_R$, and $C_p{}' = C_p + C_{in}{}^T$.

Equation 13 is equivalent to the first condition of Barkhausen. Its solutions Ω are called *zero-phase frequencies of the oscillator*.

The second Barkhausen condition can be replace by $|A_L| \geq 1$, since it was observed experimentally that the saturation of the operational transconductance amplifier limited the amplitude of the oscillation and still allowed a completely normal and predictable behavior of the microbalance circuit. For a zero-phase frequency, Ω, the modulus of the open-loop gain is given by (cf. eqs 7, 13)

$$|A_L(\Omega)| = |g_m| \frac{C_R\Omega}{|\mathrm{Im}(Y_2Y_3) + \mathrm{Im}(Y_1Y_3) + \mathrm{Im}(Y_1Y_2)|} \quad (15)$$

that is,

$$|A_L(\Omega)| = \frac{|g_m|C_R\Omega[R_m{}^2 + X_m{}^2(\Omega)]}{|G_{out}{}^T[(C_R + C_p{}')\Omega(R_m{}^2 + X_m{}^2(\Omega)) - X_m(\Omega)] + R_m[\Gamma_F(\Omega) + C_R\Omega]|} \quad (16)$$

The second condition of oscillation is $|A_L(\Omega)| > 1$, where Ω is a zero-phase frequency of the oscillator.

Derivation of the Microbalance Frequency. Equation 14 has three solutions in ω (resolution shown in Supporting Information − Section I). Only two of these solutions depend on the quartz and are associated with the zero-phase frequencies of the quartz, Ω_s and Ω_p. The third solution of eq 14 is determined by the other components of the electronic circuit. The upper zero-phase frequency of the oscillator, associated with Ω_p, upper zero-phase frequency of the resonator, is the microbalance frequency, because this frequency satisfies both conditions of Barkhausen, which is

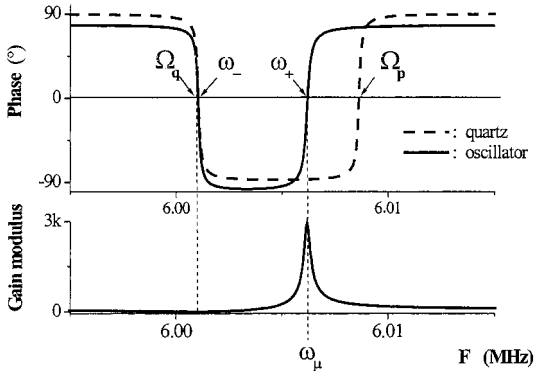

Figure 3. Phase and modulus of the open-loop gain for a 6 MHz quartz crystal resonator.

not true for the second solution associated with the quartz (cf. Figure 3; for calculations, see Supporting Information, Section II).

The microbalance frequency of the oscillator has the following expression with respect to the series frequency

$$\omega_\mu = \omega_s + \frac{1 - \bar{C}_{pq}\omega_s(\bar{C}_{pq}\omega_s {R_m}^2 - \Phi R_m)}{2L_m\bar{C}_{pq}\omega_s} \qquad (17)$$

where

$$\bar{C}_{pq} = C_p' + \frac{\Gamma_{Fq}}{\Gamma_{Fq} + C_R\omega_s}C_R$$

$$\Gamma_{Fq} = C_F'\omega_s - \frac{1}{L_F\omega_s}$$

and

$$\Phi = \frac{{G_{out}}^T}{\Gamma_{Fq} + C_R\omega_s} \qquad (18)$$

The quantity Φ depends only on the electronic components of the driving circuit and is called here the *influence factor of the electronic circuit*. The microbalance frequency can be written as follows:

$$\omega_\mu = \omega_s\left(1 + \frac{1}{2\bar{r}} - \frac{\bar{r}}{2Q^2} + \frac{\Phi}{2Q}\right) \qquad (19)$$

where

$$\bar{r} = \frac{\bar{C}_{pq}}{C_m} \qquad (20)$$

and Q is the quality factor of the quartz.

$$Q = \frac{L_m}{R_m}\cdot\omega_s \qquad (21)$$

When $R_m = 0$ (ideal quartz without losses), the microbalance oscillates at a frequency such as

$$\omega_\mu = \omega_s\left(1 + \frac{1}{2\bar{r}}\right)$$

This frequency is generally very close to the parallel frequency, ω_p, of the crystal (cf. eq 4).

$$\omega_p = \omega_s\left(1 + \frac{1}{2r}\right)$$

where

$$r = \frac{C_p}{C_m}$$

So the oscillator works at its upper zero-phase frequency, that is, close to the quartz parallel frequency, ω_p. By analogy, this type of oscillator has been called a parallel oscillator.

Limit of Microbalance Operation and Critical Motional Resistance of the Oscillator. When the load on the quartz increases, the relative variation of the motional resistance is often much higher than the relative variation of the series resonance frequency. The oscillator operation is limited by a critical value of the motional resistance, R_m. When R_m increases, the quartz zero-phase frequencies, Ω_s and Ω_p, converge and finally vanish (cf. eq 5). A *critical motional resistance of the quartz*, $R_{mc}°$, can be defined thus:[17] for $R_m < R_{mc}°$, both frequencies Ω_s and Ω_p exist, but not when $R_m > R_{mc}°$. D. M. Soares et al.[17] have proposed that an ideal oscillator, which follows Ω_s or Ω_p, ceases to oscillate when R_m becomes higher than $R_{mc}°$, such as (when the parallel capacity C_p is not compensated, e.g. by a parallel inductance)

$$R_{mc}° = \frac{1}{2C_p\omega_s} \qquad (22)$$

In practice, the components of the electronic circuit are involved in the microbalance frequency (cf. eq 17) as well as in the oscillator working limit. Beyond a critical value R_{mc} of R_m, the oscillator frequency shifts to a rest frequency, ω_{rest}, which cannot be used to study the variations of the quartz properties. Conversely, as long as $R_m < R_{mc}$, the oscillator is controlled by the variations of the quartz parameters. This critical value of the motional resistance has the following expression (see Supporting Information, Section I)

$$R_{mc} = \frac{\Phi + \sqrt{1 + \Phi^2}}{2\bar{C}_{pq}\omega_s}$$

where

$$\Phi = \frac{{G_{out}}^T}{\Gamma_{Fq} + C_R\omega_s} \qquad (23)$$

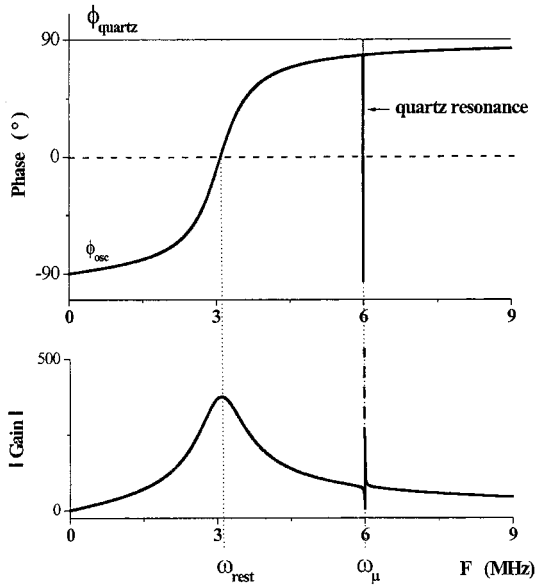

Figure 4. Phase and modulus of the open-loop gain for a 6 MHz quartz crystal resonator in a wide frequency range.

This expression is formally close to the one proposed by D. M. Soares et al.[17] (cf. eq 22), $R_{mc}°$, obtained from a quartz alone; however, eq 23 suggests that it may be possible to find electronic configurations allowing microbalance working condition beyond the critical motional resistance of the quartz, $R_{mc}°$. However, values for Φ that are too high may lead to a nonnegligible error on the mass measurement, as indicated at the end of the theoretical part. The parameter R_{mc}, called here *critical resistance of the oscillator*, depends on the values of the electronic components C_F, L_F, and C_R. So when the motional resistance of the loaded quartz crystal is known, it is generally possible to choose appropriate values for C_F, L_F, and C_R to enlarge the microbalance oscillator operating range.

In the following parts, the designation *critical point* is used to refer to the limit of the oscillator operating range, that is, $R_m = R_{mc}$.

Rest Frequency. The existence of a third zero-phase frequency was mentioned before. This frequency, referred to here as rest frequency, ω_{rest}, depends on the values of the filter components and the reaction capacitance. ω_{rest} satisfies both Barkhausen conditions (see Supporting Information, Section II). This implies that the rest frequency is also a possible oscillation frequency of the circuit (cf. Figure 4). When the motional resistance of the quartz becomes higher than the critical motional resistance of the oscillator, the microbalance frequency vanishes (cf. Figure 5) and the circuit oscillates at the rest frequency, which is equal (see Supporting Information, Section I) to

$$\omega_{rest} = \frac{1}{\sqrt{L_F(C_F' + C_R)}}$$

that is,

$$\omega_{rest} = \omega_F\sqrt{\frac{C_F'}{C_F' + C_R}} \qquad (24)$$

Influence of the Motional Resistance on the Microbalance Frequency. Equation 17 indicates that the microbalance frequency depends on the motional resistance. So a variation of this resistance causes a shift of the oscillator frequency. During metal electrodeposition, the motional resistance of the quartz generally increases as a result of energy losses in the deposited material.[7] The shift, $\Delta\omega_s$, of the series frequency generally can be considered to be due to the mass increase alone.

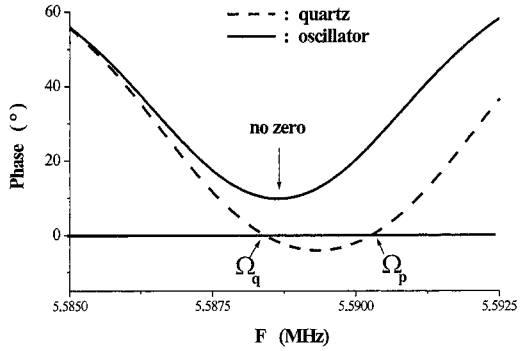

Figure 5. Absence of microbalance frequency for highly damped quartz (highly loaded 6 MHz AT-cut quartz crystal).

The shift, $\Delta\omega_\mu$, of the microbalance frequency also follows the mass variation but includes a frequency change due to the increase of the motional resistance. A quartz crystal microbalance is supposed to measure the mass variation of the film at the surface of the crystal. Therefore, the insensitivity of the oscillator to a change of the motional resistance is then a quality criterion.

A variation, ΔR_m, of the motional resistance induces a difference between the change of the quartz series frequency and the shift of the microbalance frequency. This difference can be overestimated (see Supporting Information, Section III),

$$\frac{|\Delta\omega_\mu - \Delta\omega_s|}{\omega_s} \le \frac{\Delta R_m}{R_m}\left(\frac{\bar{r}}{Q^2} + \frac{\Phi}{2Q}\right) \qquad (25)$$

where R_m and Q, respectively, are the final values of the motional resistance and the quartz quality factor.

The insensitivity of the oscillator to a variation of the motional resistance of the resonator can be discussed at the critical point in order to obtain a general estimation of the oscillator performance. At the critical point indeed, the maximum error on the mass measurement occurs. Equation 25 leads to following overestimation,

$$\frac{|\Delta\omega_\mu - \Delta\omega_s|}{\omega_s} < \frac{\bar{r}}{{Q_c}^2} + \frac{\Phi}{2Q_c} \qquad (26)$$

where Q_c is the value of the quality factor of the resonator for when $R_m = R_{mc}$.

Two limit cases related to the value of the influence factor of the circuit, Φ, may be considered:

- If $\Phi \ll 1$, then according to eq 23 and 26,

$$R_{mc} \approx \frac{1}{2\bar{C}_{pq}\omega_s}$$

$$Q_c \approx 2\bar{r}$$

and

$$\frac{|\Delta\omega_\mu - \Delta\omega_s|}{\omega_s} < \frac{1}{4\bar{r}} \qquad (27)$$

The overestimation obtained does not significantly depends on the electronic components of the circuit.

- If $\Phi \gg 1$, then according to eq 23 and 26

$$R_{mc} \approx \frac{\Phi}{\bar{C}_{pq}\omega_s}$$

$$Q_c \approx \frac{\bar{r}}{\Phi}$$

and

$$\frac{|\Delta\omega_\mu - \Delta\omega_s|}{\omega_s} < \frac{3}{2}\frac{\Phi^2}{\bar{r}} \qquad (28)$$

In this case, the maximum error on the mass measurement depends on the values chosen for the electronic components and may reach high values.

To obtain high values of the critical motional resistance of the device, one could attempt to chose a high value for the influence factor of the circuit, Φ (eq 23). The previous discussion shows, however, that this method may lead in certain cases to a significant error in the mass measurement. So the factor Φ cannot be chosen as high as possible and must take into account the frequency range and accuracy desired. A reliable oscillator is obtained for a small factor Φ and by minimizing the parasitic capacitances in parallel on the parallel capacitance of the resonator, C_p.

EXPERIMENTAL SECTION

Electrochemical Deposition and Dissolution. The oscillator behavior was studied for copper electrochemical deposition and dissolution at constant current in stirred solutions at room temperature. Electrodeposition was carried out in an acidic copper sulfate solution (0.5 mol L^{-1} $CuSO_4$ and 0.5 mol L^{-1} H_2SO_4). Under these conditions, the Faradaic efficiency has been shown to be about 96%.[19] The thickness of the copper layer was calculated using Faraday's Law.

Quartz and Crystal Holder. The experiments were based on a 6 MHz AT-cut quartz crystal with diameters of 14 mm for the crystal and 5 mm for the gold electrodes (TEMEX/CQE, France). Because the critical resistance of the oscillator (cf. eq 23) is proportional to $1/\bar{C}_{pq}$, it was important to minimize the parasitic capacities introduced in parallel with the crystal by the quartz holder and the electrical connections. Particular care was devoted to the design of the quartz holder, since it was to be used in conducting solutions. A homemade low-capacitance quartz holder was used, leading to a low parallel capacity in water: $C_p = 8.28$ pF (for the 6 MHz-quartz alone: $C_0 = 2.84$ pF). However, in the following, when the influence of the parallel capacity on the oscillator performance was studied, additional capacitances were added to the holder.

(19) Pletcher, D.; Walsh, F. *Industrial Electrochemistry*, 2nd ed.; Chapman and Hall: New York, 1989; pp 232−236.

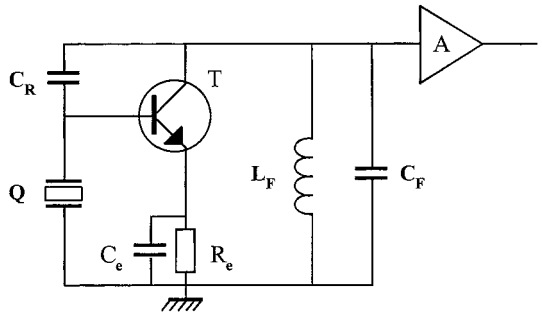

Figure 6. Schematic representation of the experimental parallel oscillator.

Oscillator. The experimental circuit is shown in Figure 6. The resistance R_e and the capacitance C_e were classically used to uncouple the transistor emitter and the ground. When the impedance of $R_e//C_e$ is small enough and its cutoff frequency is much lower than the oscillator working frequency, R_e and C_e can be replaced by a short circuit for the calculations. The values chosen for R_e and C_e were 900 Ω and 22 nF, respectively. The corresponding cutoff frequency was 8 kHz, which was much lower than the working frequency. It was experimentally observed that the oscillator could also work with a cutoff frequency much higher than ω_s, but no enhancement of the oscillator skills was noticed in this case.

T and A point out the transistor and an amplifier (buffer), respectively. Both are included in the integrated circuit OPA 660 (Burr-Brown). The transistor transconductance g_m and the output conductance $G_{out}{}^T$ depend on the value of a control resistance R_Q (connected to the OPA). R_Q was chosen to be equal to 220 Ω. This value provided a high transconductance ($g_m \approx -100$ mA/V). A high value of g_m is of practical interest when small mass variations have to be observed. The high value of the gain is responsible for steeper slopes of the output signal that triggers the frequency counter with a higher accuracy. The value of R_Q also provided a low output resistance ($R_{out}{}^T = 1/G_{out}{}^T \approx 25$ kΩ), which is the minimal accessible value for the OPA 660, according to the manufacturer data. The transistor capacities are $C_{in}{}^T = 2$ pF and $C_{out}{}^T = 4$ pF.

A ground plan partially covered each side of the circuit to minimize the parasitic coupling between the electronic components.

Electroacoustic Data. The admittance of the quartz was measured with a Hewlett-Packard 4194 A impedance analyzer. The components of the equivalent circuit were calculated using a homemade fitting program.

RESULTS AND DISCUSSION

Film Electrodeposition. Electroacoustic measurements were carried out during copper electrodeposition at a constant current equal to 26 mA/cm^2. This preliminary experiment was used as a reference, since it revealed the evolution of the quartz series frequency and motional resistance. Since the solution is stirred during deposition, its physical properties (density and viscosity) remained constant, and therefore, the series frequency variation was due only to the mass increase on the crystal surface. Because the deposition current was constant, this variation was linear (cf. Figure 7). Simultaneously, the motional resistance in solution grew

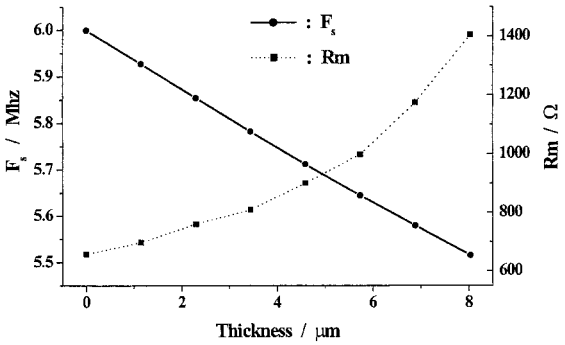

Figure 7. Quartz series frequency and motional resistance during copper electrodeposition.

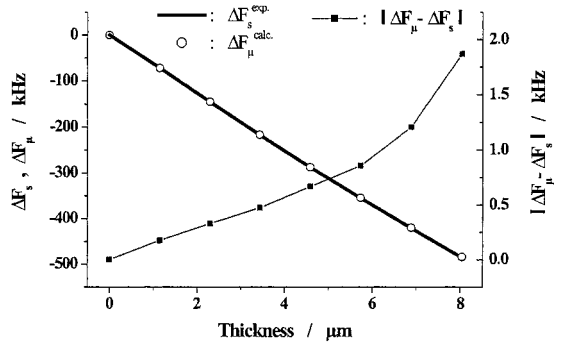

Figure 8. Predicted change of the microbalance frequency calculated from the experimental electroacoustic data.

from 660 to 1410 Ω, for a final film thickness of 8 μm. For metallic deposits, the main losses in the film seem to be due to ultrasonic wave scattering on the grain boundaries of the polycrystalline deposit.[20−22]

The error in the mass measurement induced by the increase of motional resistance was first estimated from the theory. The microbalance frequency was calculated from the electroacoustic parameters (R_m, C_m, L_m, and C_p) obtained experimentally during the deposition. The components of the experimental oscillator used for the calculation had the following values: $L_F = 390$ μH, $C_F = 1.8$ pF, and $C_R = 1.5$ pF. The corresponding value of the influence factor, Φ, was smaller than 1 and equal to 0.2. The results are shown in Figure 8. The error in the mass measurement was evaluated as follows

$$\Theta = \left|\frac{\Delta\omega_\mu - \Delta\omega_s}{\Delta\omega_s}\right| \times 100 \qquad \Theta \text{ in \%}$$

The predicted shift of the microbalance frequency very closely follows the experimental variation of the series frequency. The error was found to remain much less than 1% during the deposition. So for an experimental oscillator whose behavior is described by the analysis shown in this paper, the error induced by an increase of the motional resistance can be kept negligible during the mass increase with appropriate values chosen for the circuit components.

(20) Wunsche, M.; Meyer, H.; Schumacher, R.; Wasle, S.; Doblhofer, K. *Z. Physik. Chem.* **1999**, *208*, 225.
(21) Nicoletti, D.; Bilgutay, N.; Onaral, B. *J. Acoust. Soc. Am.* **1992**, *91*, 3278.
(22) Bhatia, A. B. *J. Acoust. Soc. Am.* **1959**, *31*, 16.

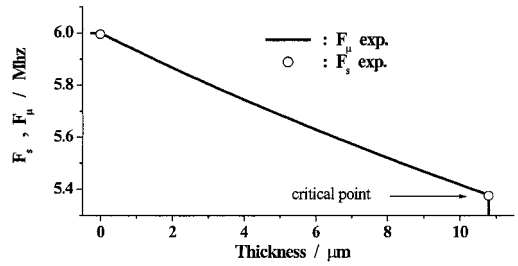

Figure 9. Experimental change of the series and microbalance frequency.

To verify that the oscillator has the expected behavior, the electrodeposition was led up to the critical point. The electroacoustic parameters were measured before and after the deposition so that the corresponding series frequency was determined. In Figure 9, the evolution of the microbalance frequency during the deposition is presented as well as the initial and final values of the series frequency. The total shift of the series frequency and that of the microbalance frequency was equal to ∼621 kHz. The error in the mass measurement was found to be smaller than 0.5%. In this experiment, because the final mass load is high for a 6 MHz quartz crystal, the variation of the series frequency was no longer rigorously linear with the mass (the film thickness was obtained from Faraday's law). Because the microbalance circuit is dependent on the series frequency, the variation of the microbalance frequency was also no longer linear. This argues for a good functioning of the microbalance device, even in the case of high mass loads.

This experiment demonstrates that the parallel oscillator presented in this paper induces no significant error on the measurement of the film mass in the case of an electrodeposition when the values of the electronic components are appropriately chosen. This remains true even in the neighborhood of the critical point.

Film Dissolution. The behavior of the microbalance was also observed during the electrochemical dissolution of a 2-μm-thick copper film. The dissolution was carried out at a 3.4 mA cm^{-2} constant current. The evolution of the motional resistance during dissolution is shown in Figure 10a. The motional resistance started to increase rapidly, reached a maximum value of ∼1.7 kΩ, and decreased. This evolution was reproducible and may be due to film stress and to a nonideally uniform decrease of the film thickness. To evaluate the influence of these large variations of R_m on the microbalance frequency, the initial and final value of the series frequency were again obtained by electroacoustic measurements. At an intermediary value of the dissolved film thickness (∼0.6 μm) at which the motional resistance was close to its maximum value, the dissolution was stopped, and an electroacoustic measurement was performed (cf. Figure 10b).

At the intermediate measurement point, the relative error between the microbalance and series frequency shifts was equal to 1.7%. At the final measurement point (∼1.3 μm), the relative error in the total dissolution was equal to 1%. These small values of the error in the mass measurement showed the reliability of the oscillator also in the case of film dissolution with large variations of the motional resistance.

Critical Motional Resistance and Oscillator Performance—Influence of the Parallel Capacitance C_p. The theory indicates

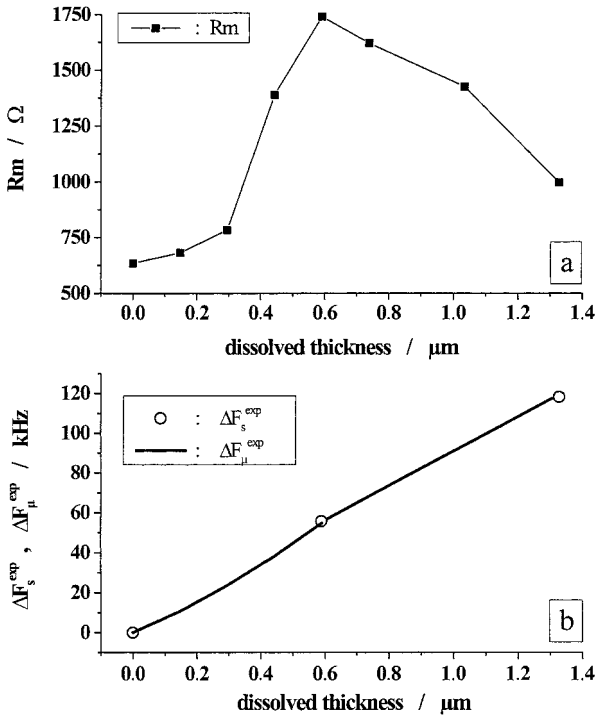

Figure 10. Changes in the dynamic resistance (a) and the series and microbalance frequencies (b) during copper electrodissolution.

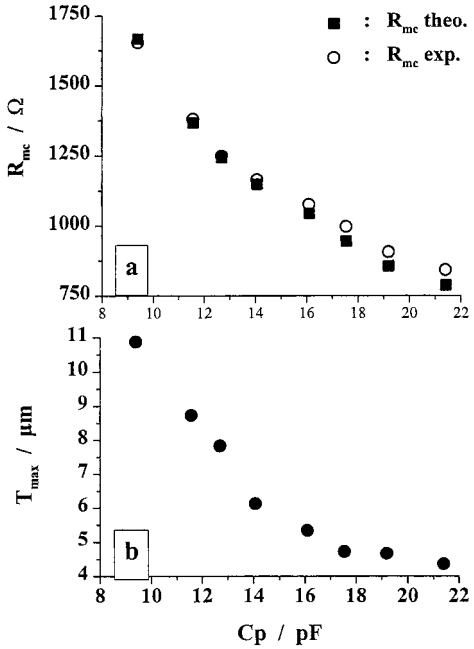

Figure 11. (a) Change in the critical resistance (theoretical and experimental) over the value of various capacitances in parallel to the quartz resonator. (b) Maximum thickness of electrodeposited copper, according to the parallel capacitance.

that the increase in the quartz motional resistance during electrodeposition limits the oscillator operation as a microbalance. The oscillator ceases to work as soon as the quartz resistance R_m reaches the critical value R_{mc}, given by eq 23. This value theoretically decreases with increasing values of the parallel capacitance of the quartz, C_p.

Capacitances with different values were connected in parallel to the quartz to artificially increase the capacitance C_p. The other components remained constant ($L_F = 390\ \mu H$, $C_F = 1.8$ pF and $C_R = 0.5$ pF). The influence factor, Φ, was equal to 0.2 (independent of C_p). For each value of C_p, copper electrodeposition was performed up to the critical point. The experimental motional resistance at the critical point was obtained from electroacoustic measurements at the end of the deposition. The results were compared to the theoretical prediction and summed up in Figure 11a. The maximum thickness T_{max} of copper that was deposited is also indicated (cf. Figure 11b, results obtained for a constant deposition courant of 26 mA cm^{-2}).

These measurements showed that the critical motional resistance rapidly decreased with increasing values of the capacitance connected in parallel with the quartz. A good agreement was found between theoretical predictions and experimental values of the critical motional resistance. The influence of C_p on the maximum thickness that can be deposited was also clearly evident. These results confirmed that the value of the parallel capacitance, C_p, due to the quartz and its holder strongly influences the oscillator performance. So in practice, care should be devoted to the design of the quartz holder and the electrical connections in order to minimize the parasitic capacitances they introduce in parallel with the crystal.

In addition, theory predicts that the cutoff frequency f_F ($f_F = \omega_F/2\pi$) of the oscillator filter does not significantly influence the critical resistance when the filter cut off and the quartz resonance do not interfere. This was also verified by using several values for the filter inductance, L_F, in order to vary the frequency (the other components remained unchanged). The predicted (R_m^{th}) and experimental (R_m^{exp}) values of the critical motional resistance versus the cutoff frequency are summed up in Table 2.

Table 2. Influence of the Filter Cutoff Frequency[a]

L_F (μH)	f_F (MHz)	R_{mc}^{th} (Ω)	R_{mc}^{exp} (Ω)
390	3.35	1667	1654
820	2.31	1616	1621
3900	1.06	1609	1598

[a] When no interference is observed with the quartz resonance.

Even if the cut off frequency varied over a large range of a few MHz, the experimental value of R_{mc} remained almost constant, with changes of only a few percent. So as analytically expected, the cutoff frequency is not the limiting parameter for the use as a microbalance when the filter cutoff and the quartz resonance do not interfere.

CONCLUSION

The experimental investigations described in this paper confirm the theoretical analysis of a parallel oscillator used as the driving circuit of a microbalance. The critical motional resistance of the oscillator determines the maximum thickness of the metal film that can be monitored on the crystal surface for a gravimetric use. In most experiments, the possibility of using the oscillator depends on the damping induced by the thin film on the quartz surface (metals, polymers) or by the surrounding medium (viscosity, density). In each case, the oscillator components have to be chosen so that the critical resistance is higher than the motional resistance induced by the film and the medium.

Moreover, the experimental results demonstrated that a change in the motional resistance has an effect on the microbal-

ance frequency that can be kept negligible when the electronic components of the parallel oscillator are appropriately chosen. In this paper, three conditions on the described circuit were proposed to obtain a microbalance that is reliable in a large domain of applications:

1. The cuff-off frequency of the filter should be chosen to be lower than the quartz series frequency and enough smaller to avoid interference with the crystal resonance.

2. The components of the electronic oscillator should be chosen so that the corresponding influence factor of the circuit is less than 1.

3. The parasitic capacitance introduced by the quartz holders and the electrical connections are to be minimized.

The use of the QCM with slightly damping films in solutions of constant physical properties during the experiment is a very common application. However, more recent applications using viscoelastic coatings, like polymers (corrosion protection, etc.) or organic layers (biodetection, etc.) may be encountered with high damping, even for very thin films. A situation in which the viscosity or the density of the solution varies during the experiment is also a well-known problem and, in many cases, a difficult one. Such situations usually require complex electronic circuits compensating for unwanted frequency variations or measuring simultaneously the damping as a second output signal. The circuit presented in this paper may not be adapted for numerous applications in which high variations of the damping at low mass variations occur.

ACKNOWLEDGMENT

H.E. wishes to acknowledge Roditech for their financial support. All the authors thank CNRS for its support.

SUPPORTING INFORMATION AVAILABLE

The following calculations are available as Supporting Information: section I, zero-phase frequencies of the oscillator (first condition of oscillation); section II, modulus of the open loop gain (second condition of oscillation); section III, influence of the motional resistance on the microbalance frequency. This material is available free of charge via the Internet at http://pubs.acs.org.

Received for review August 7, 2001. Accepted November 20, 2001.

AC010883S